

## PREDICTIVE MODELLING AND ANALYSIS OF SURFACE ROUGHNESS IN ELECTRO-DISCHARGE MACHINING OF D2 TOOL STEEL USING REGRESSION AND NEURAL NETWORKS APPROACH

Pradhan M.K.<sup>1</sup>, Das R.<sup>2</sup>, Biswas C.K.<sup>3</sup>

<sup>1,3</sup>Department of Mechanical Engineering, National Institute of Technology, Rourkela, India

<sup>2</sup>Department of Mathematics, Purushottam Institute of Engineering and Technology, Rourkela, India

Email: <sup>1</sup>mohanrkl@gmail.com

### Abstract

Surface roughness (Ra) is a significant upshot in the manufacturing process and it materializes a major part in the manufacturing system. It depends on different machining parameters and its prediction and control is a query to the researchers. In this study, a regression model and two artificial neural networks (ANNs) namely: Back propagation and radial basis function, were developed to predict surface roughness in electrical discharge machined surfaces. In the development of predictive models, machining parameters of discharge current (Ip), pulse duration (Ton) and duty cycle (D) were considered as model variables with a constant voltage 50 volt. For this reason, extensive experiments were carried out in order to collect surface roughness dataset. The developed models are validated with a new set of experimental data, and predictive behavior of models is compared, subsequently relative advantages of each model are analyzed. Analysis of variance (ANOVA) and F-test were used to check the validity of regression model and to determine the significant parameter affecting the surface roughness. The statistical analysis exemplify that the Ip, Ton and D were the factors in sequence have significant influence the on surface roughness. The microstructures of machined surfaces were also studied by scanning electron microscopy (SEM). The SEM investigations revealed that EDMed produced were increased significantly with Ip.

**Keywords:** Surface roughness, Regression analysis, Back propagation, radial basis function

### I. INTRODUCTION

With the continuous demand of components of new and advanced “difficult-to-machine” materials (tough super alloys, ceramic and composites) having stringent design necessities to fabricate complex shapes, tighter tolerance and very high machining cost, are incessantly challenging the modern manufacturing industry. These advance materials plays increasingly important role in the modern manufacturing industries, mainly in automobile, aircraft, tool, die, and mould making industries. The substantially increased properties such as strength, wear resistance, heat resistance, etc. yielded huge advantage to the manufacturing industries through superior product performance and product design. However, the traditional manufacturing processes are not capable to machine these materials inexpensively [1]. Thus, to meet up such demands, the traditional machining processes are increasingly being replaced with advance manufacturing process, which make use of distinct class of energy for material removal using the material properties, such as electrical and thermal conductivity, melting temperature, electrochemical equivalent etc. Amongst all such non-traditional machining processes, electro discharge machining (EDM) is regarded as one of the most vital processes which is suitable for a wide range of applications in the said industries. It is a thermal process of eroding electrically conductive materials with a series of repetitive electric sparks. The mechanism of erosion is a complex phenomenon concerning several disciplines of science and branches of engineering. The theories

revolving around the formation of plasma channel between the tool and the workpiece, thermodynamics of the repetitive spark causing melting and evaporating the electrodes, micro-structural changes, and metallurgical transformations of material, are still not clearly understood. However, it is widely accepted that the mechanism of material erosion is due to intense local heating of the workpiece causing melting and evaporation of workpiece. Therefore, for insight the process in a better way, extensive qualitative and quantitative analysis of the mechanism is vital and subsequently development of models, understanding the influence of various process parameters on the responses, confirmation of experimental results and enhancing the process performance by implementing/incorporating some of the theoretical findings are necessary [2].

Several research attempts has been made to model the EDM process, the interest is to recognize the effect of machining parameters on the responses. Tsai and Wang [3] developed a semi-empirical model and testify that factors spark time, maximum current, polarity, input power, material density, conductivity of the material, specific heat capacity, heat conductivity, melting point, and boiling point of the material are affecting the surface roughness. Halkacý and Erden [4] performed an experimental study and identified relations between Ra and spark time, in addition to Ra and power. Rebelo et al. [5] looked into parameters for material removal rate and Ra when processing of hard copper-berilium alloys and the effect of discharge current and discharge time on surface integrity

was presented. Petropoulos [6] presented a multi-parameter analysis of surface finish imparted to Ck60 steel plates by electro-discharge machining. The interrelationship between surface texture parameters and process parameters is highlighted.

In recent times, ANNs have materialized as a extremely flexible modeling tool for manufacturing sectors. ANNs are found to be effectual as computational processors for various associative recall, classification, data compression, combinational problem solving, adaptive control, modeling, forecasting, multisensor data fusion, and noise filtering. These competences of ANNs in capturing the mathematical mapping between input variables and responses are the driving force of implementing for modeling machining processes. The complexity and stochastic nature of EDM process has defied numerous attempts of ANN modeling it accurately.

Tsai and wang [7] demonstrated six different neural-networks models and a neuro-fuzzy network for the purpose of assessment the surface finish for different work material with the change of electrode polarity and concluded comparing the results and checking errors among these models that experimental results are in good agreement to the predictions. Assarzadesh et al. [8] offered a 3-6-4-2-size BPN model to ascertain a process model considering  $I_p$ , Ton and voltage as input to the network and MRR and Ra as output, which is able to predict process performance with reasonable accuracy, under varying machining conditions. Mandal et al. [9] attempted to model the EDM process using ANN with back propagation as the learning algorithm. Ra, MRR and tool wear, with various input parameters and found suitable for predicting the response parameters. Markopoulos [10] proposed a ANN model for the prediction of Ra using  $I_p$ , Ton, and the processed material as input parameters and found satisfactorily prediction of Ra. Pradhan [11] presented a neuro-fuzzy model to predict MRR with different process parameters such as  $I_p$ , Ton and t, and the model predictions were found to be in good agreement with the experimental results Indurkhya Gopal [12] used 9-9-2 size back propagation network with input parameters such as  $I_p$ , Ton Toff, machining depth, tool radius, orbital radius, radial step, vertical step, offset depth, etc. and material removal rate and Ra as output parameter. The results are compared with the multiple regression analysis and reported that ANN provides faster and more accurate results.

The literatures reveal that there are several attempts have been made to model the Ra with ANN, on the other hand, regression analysis is also attempted by many researchers, and however, very few attempts are on comparison between them. Apart from this, very few works

are reported on AISI D2 tool steel, which has a growing range of application on the field of mould making industries. In this work two different ANN model (BPN and RBFN) and regression have been employed, and comparison is made among them. The ANN models uses data for the training are obtained from the experiments with the input parameters  $I_p$ , Ton, and t, which varied over a wide range, from roughing to near-finishing conditions and corresponding response Ra. The model is tested with the test data that are not earlier used to develop the model. From the same set of data a second order regression model is also developed and ANOVA is used to check the sufficiency of the model. At the end of study, both the ANN and regression analysis results were compared with experimental data and prediction errors have been calculated for the testing data. The proposed models were found to be successful, for reliable predictions, which provides a possible way to avoid time and money-consuming experiments

## II. EXPERIMENTAL DETAILS

Experiments were conducted on Electronica Electraplus PS 50ZNC die sinking machine. A cylindrical pure copper was used as a tool electrode (of positive polarity) with a diameter of 30 mm and workpiece materials used were AISI D2 tool steel square plates of dimensions 15×15 mm<sup>2</sup> and thickness 4 mm. Commercial grade EDM oil (specific gravity = 0.763, freezing point = 94°C) was used as dielectric fluid. Lateral flushing with a pressure of 0.3 kg f/cm<sup>2</sup> was used. Keeping the voltage constant at 50 V, number of experiments was conducted to investigate the effects of  $I_p$ , Ton and  $\tau$  on Ra, where is defined as:

$$\tau = \frac{\text{Ton}}{\text{Ton} + \text{Toff}} \times 100 \quad (1)$$

The experimental conditions and the levels of the input parameters are shown in Table 1. Each treatment of the experiment was run for 15 minutes and the Ra was measured

**Table 1. Experimental Contortions**

Sparking voltage in V	50
Current ( $I_p$ ), in A	1 5 10 20 30 50
Pulse on Time (Ton), in s.	5 10 20 30 50 100 150 200 500 750
Duty Cycle ( $\tau$ )	1 12
Dielectric used	Commercial grade EDM oil
Dielectric flushing	Side flushing with pressure
Work material	AISI D2 tool steel
Electrode material	Electrolytic pure Copper
Electrode polarity	Positive
Work material polarity	Negative

### III. SURFACE ROUGHNESS MEASUREMENT

The Ra is used to portray the technical surface quality of an engineering component. It has very significant influence on the manufacturing outlay of a product. A good quality surface enhances the fatigue strength, corrosion, and wear-resistance of the workpiece. There is a number of ways by which surface roughness of a component is described, such as roughness average (Ra), root-mean-square (rms) roughness (Rq) and maximum peak-to-valley roughness (Ry or Rmax), etc. In this work, Ra is used, which is measured using Talysurf (Taylor Hobson, Surtronic 3+). The profilometer was set to a cut-off length of 0.8 mm, filter 2CR, traverse speed 1 mm/second and 4 mm evaluation length. Roughness measurements, in the transverse direction, on the workpieces were repeated four times and average of four measurements of surface roughness parameter values was recorded. The measured profile was digitized and processed through the dedicated advanced surface finish analysis software Talyprofile for assessment of the roughness parameters. Ra can be defined as the arithmetic value of the profile from centerline along the sampling length. It can be expressed as

$$Ra = \frac{1}{L} \int |y(x)| dx \quad (2)$$

Where L is the sampling length, y is the profile curve and x is the profile direction. The average Ra is measured within L = 0.8 mm. Centre-line average Ra measurements of electro-discharge machined surfaces were taken to provide quantitative evaluation of the effect of EDM parameters on surface finish.

### IV. PREDICTIVE MODELS FOR SURFACE ROUGHNESS

#### A. Regression Analysis

A second order polynomial regression model for three variables under consideration is proposed. The equation for Ra can be written as shown in Equation 3.

$$Ra = a_0 + a_1 I_p + a_2 T_{on} + a_3 t + b_1 I_p^2 + b_2 (T_{on})^2 + b_3 t^2 + c_1 I_p T_{on} + c_2 T_{on} t + c_3 I_p t \quad (3)$$

The co-efficient  $a_0$  is the free term; the coefficients  $a_1$ ,  $a_2$  and  $a_3$  are the linear terms; the coefficients  $b_1$ ,  $b_2$  and  $b_3$  are the quadratic terms; and the coefficients  $c_1$ ,  $c_2$ , and  $c_3$  are the interaction terms. The coefficients of regression model were estimated from the experimental results and the model is developed.

ANOVA is used to check the sufficiency of the second-order model, which includes test for significance of the regression model, and model coefficients. It is used for

testing the null hypothesis of the experimental data with a confidence level of 95%. The p-value for the F-statistic, expressing the probability of observing a value of F at least, as large, if  $H_0$  is true and treatments have no effect. If p-value less than 0.05, it is concluded that  $H_a$  is true and the treatments have a statistically significant effect. Ra obtained from the experiments is compared with the predicted value calculated from the model. Table 2 is an ANOVA summary of the terms in the model, corresponding coefficients (Coef.) of the terms, the standard error of a coefficient (SE Coef), t-statistic and p-value of the terms to help to decide whether to reject or fail to reject a null hypothesis. It can be seen that the p-value of all the terms are below the  $\alpha$ -value, hence they are significant in the model. The values of  $R^2$  and  $R^2_{adj}$  are 96.9% and 96.4%, respectively. Where  $R^2 = 96.9\%$  indicates that 96.9% of total variation in the response that is explained by predictors or factors in the model and  $R^2_{adj}$  is 96.4%, which accounts for the number of predictors in the model describes the significance of the relationship.

Table 2. ANNOVA Summary

Term	Coef	SE Coef	T	P
Constant	2.11660	0.371989	5.690	0.000
$I_p$ (A)	0.26529	0.058142	4.563	0.000
$T_{on}$ ( $\mu$ S)	0.04311	0.004804	8.972	0.000
t	-0.08958	0.040347	-2.220	0.034
$I_p * I_p$	-0.00286	0.000988	-2.895	0.007
$T_{on} * T_{on}$	-0.00004	0.000006	-7.148	0.000
S = 0.9851 R-Sq = 96.9% R-Sq(adj) = 96.4%				

Table 3 illustrates the ANOVA analysis of the model, and the columns describing the degrees of freedom (DF), the sequential sums of squares (Seq SS), the adjusted sums of squares (Adj SS), the adjusted means squares (Adj MS), the F-statistic from the adjusted means squares, and its p-value. The sequential sum of squares is the added sums of squares given that prior terms are in the model, which depends on the model order. The adjusted sums of squares are the sums of squares given that all other terms are in the model that does not depend upon the model order. It can be observed in this table, the p-value of regression model is less than 0.05, hence, the Ra fitting the regression model with the linear, and square terms are significant at the level of 95%. The square terms of along with all interaction terms are not included in the model as their p-values are exceeding the  $\alpha$ -value. This way the simplified truncated model is shown in the following equation.

$$Ra = 2.1166 + 0.26529 Ip + 0.04311Ton - 0.08958 t - 0.002861 p^2 - 0.00004 Ton^2$$

**Table 3. The ANOVA table for the fitted models.**

Source	DF	Seq SS	Adj SS	Adj MS	F	P
Regression	5	880.88	880.88	176.176	181.55	0.000
Linear	3	796.78	274.49	91.499	94.29	0.000
Square	2	84.09	84.099	42.049	43.33	0.000
Residual Error	29	28.141	28.141	0.9704		
Total	34	909.02				

### B. Neural Network Modeling

An ANN is a new computing tool that process information using neurocomputing approach. This is different from the classical computation. In past, several studies have been reported on the development of neural networks based on different architectures. Neural networks are characterized by their architecture, activation function and learning algorithms. Each type of neural networks would have its own input-output characteristics, and therefore it could be applied only on some specific process.

A neural network is represented by weighted interconnections between processing elements. These weights are the parameters that actually define the non-linear function performed by the neural network. The process of determining such parameters is called training or learning, relying on the presentation of many training patterns.

The architecture of the neural network having n inputs and m outputs is given in the Figure. 1.

In this study, two neural networks are used for modeling the Ra in the EDM process. Two networks are discussed as follows.

1. Back-propagation Neural Network (BPNN)
2. Radial basis function neural network (RBFNN)

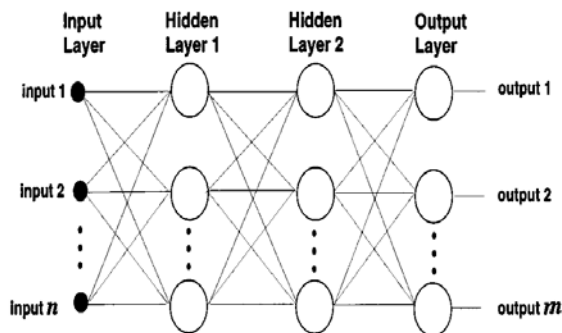


Fig. 1. Architecture of Neural Network

**Table 4. Description of BPNN**

	Input	Hidden	Output
Number neurons	$n+1$	$m+1$	$r$
Function	linear	sigmoidal	Sigmoidal
Neuron index range	$i=0, \dots, n$	$h=0, \dots, m$	$j=0, \dots, r$
Activation	$x_i$	$z_h$	$y_j$

### 1. Back-propagation Neural Network

Back-propagation networks are composed of layers of neurons. The input layer of neurons is connected to the output layer of neurons. The network has the general architecture as shown in Fig. 1. Input layer neurons are linear, whereas neurons in the hidden and output layers have sigmoidal functions.

Vector or scalar variables will be subscripted or superscripted by the iteration index, k. All neurons use similar functions. For linear neurons in the input layer,

$$S(x) = x$$

and for sigmoidal neurons in the hidden and output layers,

$$S(x) = \frac{1}{1 + e^{-x}}$$

We assume a set of Q training vector pairs:

$$T = \{(X_k, D_k)\}_{k=1}^Q$$

$X_k \in R^n$   $D_k \in R^r$  where  $D_k$  is a vector response desired when input  $X_k$  is presented as input to the network.

The vector pairs in T are assumed to be samples representative of some unknown function  $f: R^n \rightarrow R^r$

which we wish the neural network to approximate. The error gradient for a pattern are computed and used to change the weights in the network. For kth training pair

$(X_k, D_k)$  then define the error.

$$E_k = D_k - S(Y_k)$$

and

$$\epsilon_k = \frac{1}{2} E_k^T E_k$$

where  $\epsilon_k$  is the sum of the squares of the each individual output error. The mean square error  $\epsilon$ , is computed over the entire training Set T on a specific neural network.

$$\epsilon = \frac{1}{Q} \sum_{k=1}^Q \epsilon_k$$

The error calculated is used to compute the change in the hidden to output layer weights and the change in input to hidden layer weights such that a global error measure gets reduced. Then all weights of the network are updated. It will be repeated until the global error falls below a predefined threshold.

#### Radial Basis Function Neural Network

Through a defined learning algorithm, the network performs the adjustments of its weights so that error between the actual and desired responses is minimized. Once trained, the network performs the interpolation in the output vector space. In the previous section we discussed that back propagation network can be trained to perform a nonlinear mapping between the input and output vector spaces. In this section we present an alternative network that is capable of accomplishing the same task. This is the radial basis function neural network.

RBFNN is based on supervised learning. It consists of three layers: an input layer, a single layer of nonlinear processing neurons, and output layer. Input layer contains  $n$  neurons and output layer contains  $r$  neurons. It has a feed forward structure consisting of a single hidden layer of  $m$  locally tuned units which are fully interconnected to an output layer of  $r$  linear units. All hidden units simultaneously receive the  $n$ -dimensional real valued input vector  $X$ . The main difference from that absence of hidden layer weights. RBFNNs are best suited for approximating continuous or piecewise continuous real valued mapping  $f: R^n \rightarrow R^r$

when  $n$  is sufficiently small. RBFNN can be viewed as approximating a desired function  $f(x)$  by superposition of non orthogonal, bell-shaped basis functions. The degree of accuracy of these RBFNN can be controlled by three parameters: the number of basis functions used, their location and their width.

In the present work we have assumed a Gaussian basis function for the hidden units given as  $Z_j$  for  $j = 1, 2, \dots, M$

Given an input vector  $X$ , the output value  $O_k(X)$  of the  $K$ th output node is equal to the sum of the weighted outputs of the hidden nodes and the bias of the  $k$ th output node and is described by

$$Z_j = \exp\left(-\frac{\|X - \mu_j\|^2}{2\sigma_j^2}\right)$$

where  $W_{kj}$  is the weight between the  $j$ th hidden node and  $k$ th output node.

The sum of the squared error function can be considered as an error function  $E$  to be minimized over the given training set. The training of the RBFNN is radically

different from the classical training of standard feedforward neural network. In this case, there is no changing of weights with the use of the gradient method. In RBFNN with the chosen type of radial basis function training resolves itself into selecting the center and width and calculating the weights of the output neurons. Heuristic operation on a given defined training set starts from an empty subset of the basis function. Then the empty subset is filled with succeeding basis functions with their center marked by the location of elements of the training set. It decreases the sum-squared error or the cost function. In this way, a model of the network constructed each time is being completed by the best element. Construction of the network is continued till the criterion demonstrating the quality of the model.

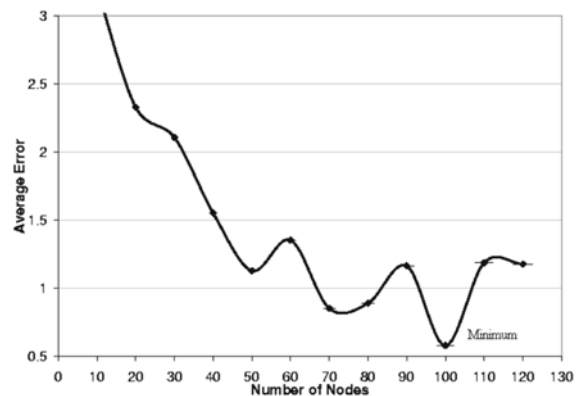


Fig. 2. Comparison of average errors for various nodes on BPNN

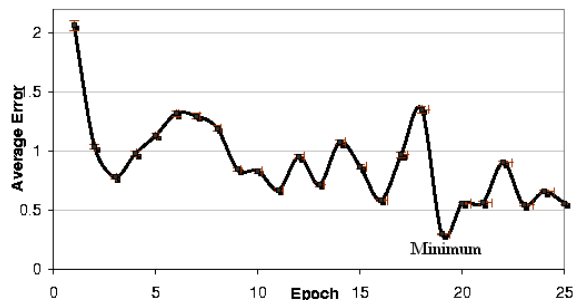


Fig. 3. Comparison of average errors for various epochs on BPNN

Initially, the architecture and the topology of the networks i.e. the number of hidden layers and the number of neurons in each layer in the networks are decided. The process parameters the discharge current ( $I_p$ ), pulse on time ( $T_{on}$ ), duty cycle ( $t$ ) and Voltage ( $V$ ) are taken as the inputs and  $R_a$  is taken as output. Thus, there are four input nodes and one output node. The variation of process

parameters for different experimental set (Run) are as presented in the Table 1.

The size of the network becomes very large for large number of training patterns. As such, the data for training is selected judiciously. 35 training data sets are considered for both the networks to compare the performances. Besides, 9 testing sets outside the training data set are selected for testing the neural networks. The training data sets and the test data sets are taken from Experiment. Both the ANNs were trained with the above datasets to reach the error goal. The performance of two neural network models is studied with the special attention to their generalization ability and the training time

It is a difficult task to find an optimal configuration of BPNN. There are no exact rules for setting the proper number of neurons in the hidden layer to avoid over fitting or under fitting to make the learning phase convergent. For the best performance of the BPNN, the proper number of nodes in the hidden layer is selected through a trial and error method based on the number of epochs needed to train the network. It was observed that the network performed well with 100 nodes and 500 epochs.

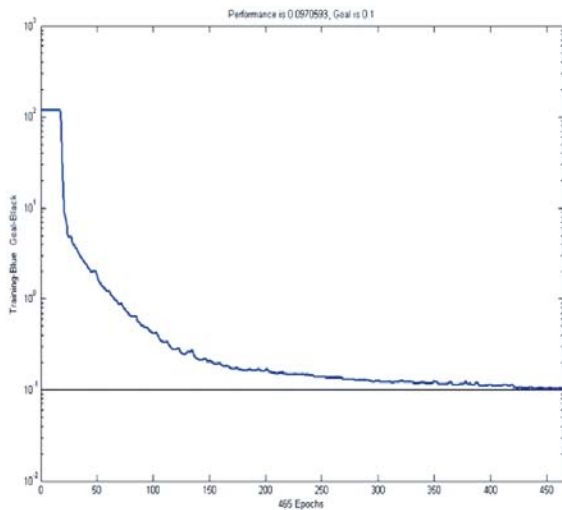


Fig. 4. Learning behavior of BPNN model for surface roughness

The learning behavior of BPNN model for Ra is shown in Figure 5. The RBFN is auto configuring in the sense that it has only one hidden layer with a growing number of neurons during learning to achieve an optimal configuration. The only parameter to be varied to obtain the best generalization ability is the spread factor (SF). Computations are carried out for different values of spread factor. It was observed that the best generalization ability of the network achieved with a spread factor of value 45 (Figure 6).

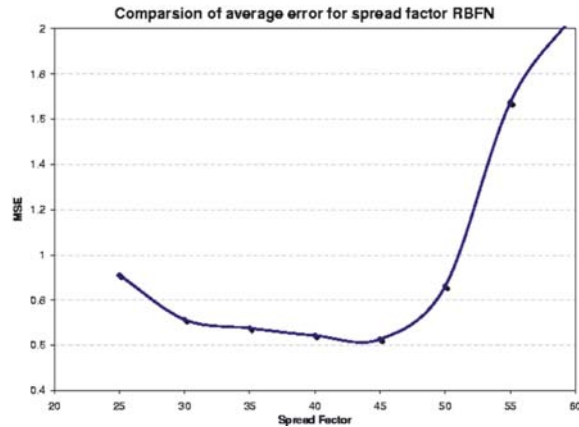


Fig. 5. Comparison of average error for various nodes and spread factor.

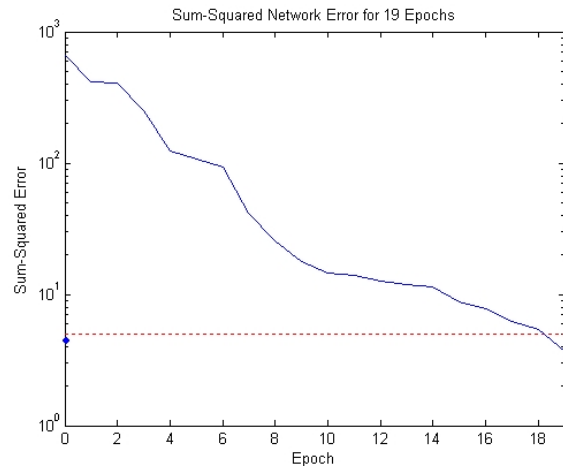


Fig. 6. Learning behavior of RBFN model for surface roughness

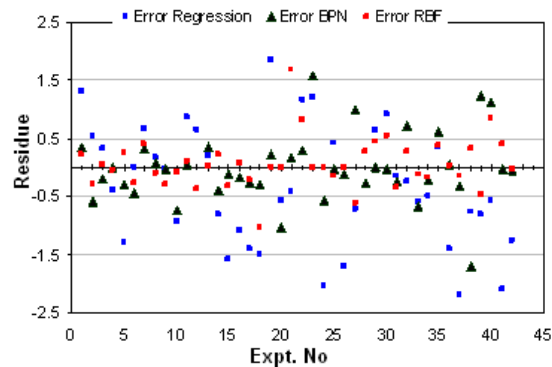


Fig. 7. Plot of residuals vs. Expt No.

The training performances of the same training data sets are shown in Fig.7. The error goal is reached in only 19 epochs in RBFN, while 500 epochs are required by the BPNN. Fig. 7 displays the normal probability plot of the residuals, which is used to test the normal distribution of the errors

The distribution of independent random errors of observation is expected to take a normal distribution. It can be seen that the residuals are almost falling on a straight line, which indicates that the errors are normally distributed.

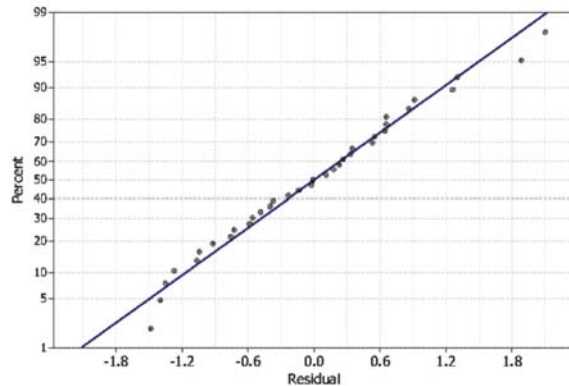


Fig. 8. Normal plot of residuals.

The plot of the residues verse expt. number for the model under consideration are illustrates that the errors are distributed randomly as there is no noticeable pattern or unusual structure present in the data as depicted in Fig. 8, it suggests that the models fit the data well. Also the residuals which are very large or very small than the rest are typically called outlier and a few such outliers may distort the analysis. The residues, which are calculated as the difference between the predicted and observed value lies in the range of  $-2.2$  to  $1.86$ ,  $-1.77$  to  $2.65$  and  $-1.04$  to  $1.69$  for regression, BPN and RBFN respectively.

Experimental observation is compared with the predicted values of each model, regression, BPN and RBFN in the Fig. 9 to demonstrate the accuracy of the predictive model. The represented data refer to both training and validation data sets. These plots are also presented straight lines to make them easier to infer. It is seen that the predicted and experimental values in the models could predict very accurately and except for one or two outlier, almost all the values are close to the line. It could be noted that closer the value to the line, more is the accuracy. The three lines match fairly closely for lower values of Ra. However, for large values of Ra, the Regression line tends to generate higher values for the predicted values than does the BPN and RBFN. BPN and RBFN are similar at all the ranges, nevertheless the RBFN model is comparatively more accurate than the BPN and regression model, having correlation co-efficient  $0.998$ ,  $0.988$  and  $0.978$ , respectively, which conforms the effectiveness of the models and that all the three models are moderately well fitted with the experimental value. However, the models can be sequenced as regression, BPN and RBFN, respectively, in terms of accuracy.

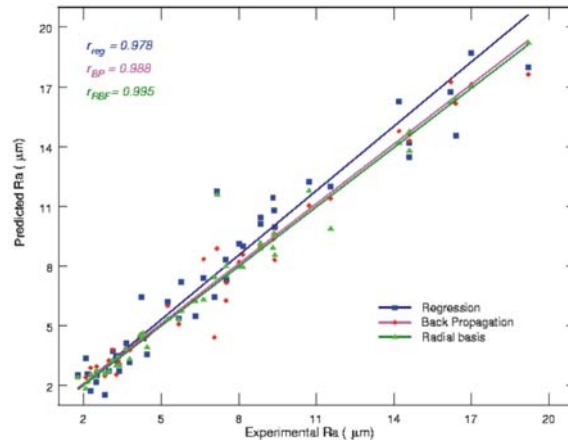


Fig. 9. Predicted vs. experimental Ra the correlations coefficients.

## V. PREDICTION ERROR

The validation of all the models is carried out with the testing data set that is not previously used to develop the model. In order to assess the accuracy of the prediction models, percentage error and average percentage error are used. Prediction error has been defined as follows

$$\text{Prediction error} = \frac{|\text{Expt. MRR} - \text{Fitted MRR}|}{\text{Expt. MRR}} \times 100 \quad (4)$$

In Table 5, the process parameters of testing data, their corresponding experimental Ra, percentage error and the average percentage error are shown. The average percentage error of these model validations are about  $4.11\%$ ,  $9.01\%$ , and  $20.21\%$  for RBF, BPN, and regression model, respectively. Consequently, the models can be sequenced as RBFN, BPN, and regression model, in terms of prediction accuracy.

ANNs are compared separately with results obtained by experiments and the average error obtained for both the networks. RBFN model is poorer at two input values but for the rest of the input range, within which the normal operating range lies, both the models have almost identical generalization ability. The test results accuracy measured in terms of mean absolute error (MAE) for 7 test data are found to be  $0.297188$  for the BPNN and  $0.574888$  for RBFN. In the case of RBFN, the number of epochs is equal to the number of neurons in the single hidden layer of the network. The error goal is reached in only 19 epochs, while 465 epochs are required by the BPNN. The amount of the work done in each epoch is not equivalent for both ANN's.

Figure 11 shows the error for each model, calculated as the difference between the experimental findings and predicted values. It was found that except at two places, both the models predict the roughness.

**Table 5. Test data and Prediction errors**

Sl.No	Ip (A)	Ton (µs)	$\tau$	Ra (µm)	%Error Reg	%error BPN	%error RBFN
1	5	100	1	5.78	-24.45	0.73	0.55
2	10	50	1	4.24	-52.11	-7.68	-3.21
3	10	75	1	6.64	-11.48	-25.61	4.97
4	10	100	1	7.5	-10.73	16.56	-6.36
5	10	150	1	9.4	-5.96	11.77	9.06
6	10	200	1	9.32	-22.49	-0.13	4.38
7	20	100	1	8.84	-14.25	-0.59	-0.22
Average prediction error					20.21	9.01	4.11

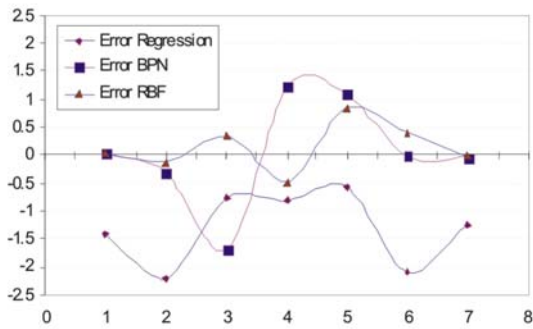


Fig. 10. Residuals calculated as the difference between experimental and predicted values for the data set.

The test data and prediction error is shown in Table-4. The process variables and the experimental Ra are. In order to evaluate the accuracy of the prediction model, percentage errors are used. Percentage of prediction errors is shown in the in the Table. It can be noted that the RBFN is the best while predicting the Ra with 9.06 % prediction error. However, the other two models are also predicting the Ra except at one or two outliers. The experimental results and predicted results of 'Ra' by the BPN and RBFN were plotted on the same scale, as shown in figure 9.

**VI. CORRELATION BETWEEN SURFACE ROUGHNESS AND MACHINING PARAMETERS**

**A. Effect of Ip**

To establish the effect of EDM on the Ra of the AISI D2 steel, the surface profiles of the topography of the EDM surfaces were measured.

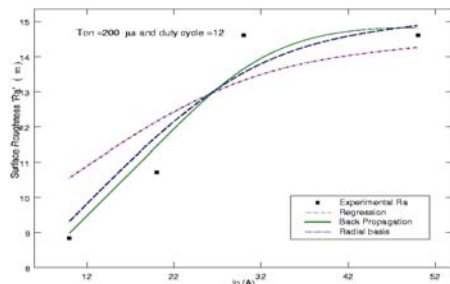


Fig. 11 Effect of Ip on Ra

Figure 11 shows the measurement results. The Ra on the machined surface varied from 8 µm to 17µm. The higher pulsed current caused more frequent melt expulsions, leading to the formation of a deeper and larger crater on the surface of the workpiece and resulted in a poorer surface finish

**B. Effect of Ton**

The effect of pulse duration (Ton) on Ra is depicted in Fig. 12 and 13 for Ip = 20, and 30 A respectively. It can be observed that the Ra increases steadily with the increase in Ton. This increase in Ra is sharper for Ip=30 than that of Ip=20, where it shows a peak after which Ra decreases. It is expected that when the pulse time increases, the Ra usually increases up to a maximum value after which it starts to decrease. The higher pulsed current caused more frequent melt expulsions, leading to the formation of a deeper and larger crater on the surface of the workpiece and resulted in a poorer surface finish. With the further increase of Ton the bigger and shallow craters are formed and therefore the Ra decreases.

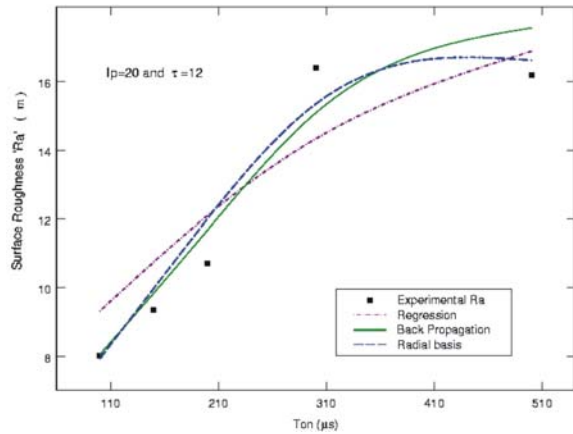


Fig. 12. Effect of Ton on Ra at Ip= 20 and τ=12

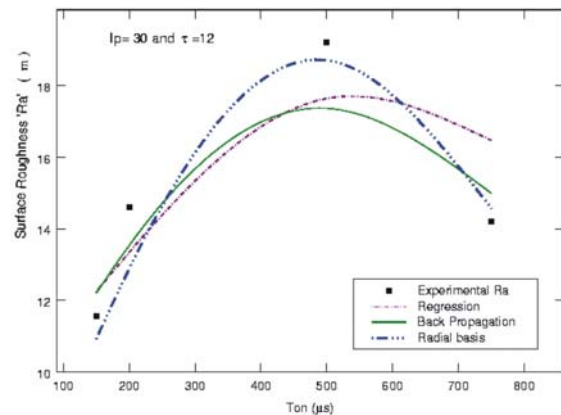


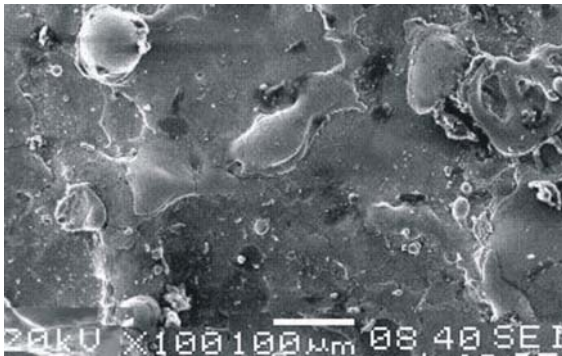
Fig. 13. Effect of Ton on Ra at Ip= 30 and τ=12



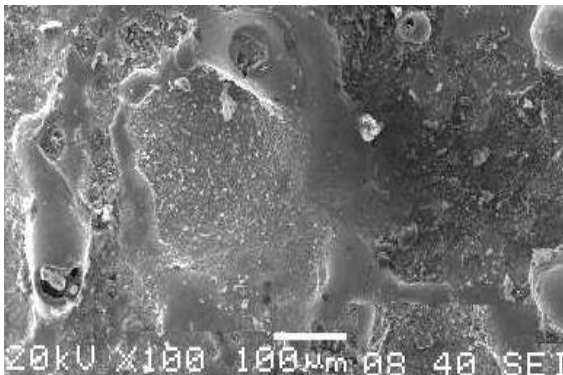
Comparing with the results of Fig. 2 and Fig. 6, we find that good machined finish can be obtained by setting the machine parameters at low pulsed current and small pulse-on-duration, but that will be more time consuming.

#### VII. ANALYSIS SURFACE ROUGHNESS USING SEM

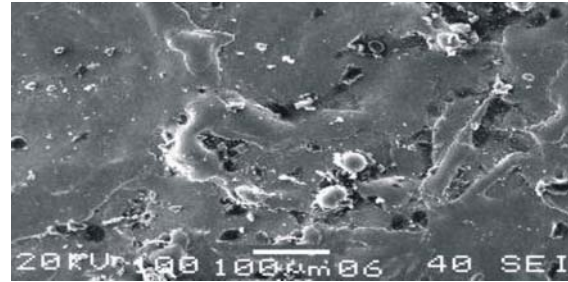
The EDMed surfaces of AISI D2 tool steel were examined using the SEM and depicted in the Figs. 14 (a)-(c). Figure 14(a) represents the surface generated when EDMed with  $I_p=10$ , however Figure 14(b), with  $I_p=20$  and figure 14(c), with  $I_p=30$ . With the increase in  $I_p$  the spark energy increases, and hence forms bigger craters. The diameter and the depth of craters of the EDMed surface increase with an increase in the discharge current, and hence the  $R_a$  consequently increases. Significantly different  $R_a$  value with the change in  $I_p$  is represented by these three samples. The size of the crater can be clearly visualized with the increasing discharge current. In the SEM micrographs bigger craters due to larger amount of molten work-material with the spark erosion can be identified on EDM surfaces.



(a)  $I_p = 10$



(b)  $I_p = 20$



(c)  $I_p = 30$

Fig. 14. SEM of EDMed surfaces of AISI D2 Steel

#### VIII. CONCLUSION

In this research, a large number of experiments have been accomplished with a wide range of current, pulse on time and duty cycle. The surface roughness has been assessed for each setting of current, pulse on time and duty cycle. Surface roughness values are predicted using a regression model and two artificial intelligence techniques: namely BPNN and RBFN. The resulting predictions are compared with the experimental results from the EDM process done on the AISI D2 steel materials with different machining parameters using copper electrode. The proposed prediction networks are validated with the experimental results and also comparison was made among them. The following is the outcome of this study:

1. The regression model is quite comparable to the ANN models for prediction of  $R_a$  and they can provide a satisfactory prediction. The predicted process parameters on validation are found to be close correlation with the actual experimental results. It is seen that ANN provides the better prediction capability with coefficient of correlation 0.988 and 0.995 respectively for BPN and RBFN, while 0.978 for regression model. Though the proposed regression model is adequate and accepted, neural network models yield better prediction
2. The evidence of correct prediction is also proved by the mean prediction error is as low as 3.06%, 9.01% and 20.21% for RBFN, BPN and regression model respectively.
3. The BPNN showed a slightly better performance compared to the RBFN model i.e. the MAE for test data are 0.297188 for the BPNN and 0.574888 for RBFN. However, the RBFN model predicts quite faster the error goal reached in only 19 epochs while BPNN requires 500 epochs. It is important to note that for BP networks the required number of nodes in the hidden

layer was found by trial and error method, where as, the RBFNs have only one hidden layer with a growing number of neurons. The overall outcome is that the surface finish of EDMed surface can be predicted by the above models with reasonably better accuracy.

4. The surface roughness is found to increase with the increase in discharge current, however it increases to a optimum value and then start decreasing with the increase in pulse on time.

### REFERENCES

- [1] Snoeys, R., Staelens, F., Dekeyser, W., 1986, Current trends in nonconventional material removal processes. *Ann. CIRP* 35(2), 467-480
- [2] Jain NK, Jain VK, 2001, Modeling of material removal in mechanical type advanced machining processes: a state-of-art review. *Int J Mach Tools Manufact* 41(11):1573–1635
- [3] Tsai K, Wang P, 2001, Semi-empirical model of surface finish on electrical discharge machining. *Int J Mach Tools Manuf* 41(10):1455–1477
- [4] Halkaci H S, Erden A, 2002, Experimental investigation of surface roughness in electric discharge machining (EDM). 6th Biennial Conference on Engineering Systems Design and Analysis, Y" stanbul, Turkey, 8–11.
- [5] Rebelo JC, et al, 2000, "An experimental study on electro-discharge machining and polishing of high strength copper–beryllium alloys". *J Mater Process Technol* 103:389–397.
- [6] Petropoulos, G., Vaxevanidis, N. M., & Pandazaras, C, 2004, Modeling of surface finish in electro-discharge machining based upon statistical multi-parameter analysis. *Journal of Materials Processing Technology*, 155–156, 1247–1251.
- [7] Tsai K-M, Wang P-J, 2001, Predictions on surface finish in electrical discharge machining based upon neural network models. *Int J Mach Tools Manufact* 41(10):1385–1403.
- [8] S.Assarzadeh, M. Ghoreishi, 2007, Neural network based modeling and optimization of the electro-discharge machining process, *Int J Adv Manuf Technol*.
- [9] Debabrata Mandal Surjya K. Pal Partha Saha, 2007, Back propagation neural network based modeling of multi-responses of an electrical discharge machining process *International Journal of Knowledge-based and Intelligent Engineering Systems* Volume 11, Issue 6, pp 381-390.
- [10] Markopoulos, A.P. Manolakos, D.E. Vaxevanidis, N.M, 2008, Artificial neural network models for the prediction of surface roughness in electrical discharge machining, *Journal of Intelligent Manufacturing*, Volume 19, No. 3 .
- [11] Pradhan, M. K. and Biswas, C. K, 2008, Neuro-fuzzy model on material removal rate in electrical discharge machining in AISI D2 steel. *Proceedings of the 2nd International and 23rd All India Manufacturing Technology, Design and Research Conference*, 1: 469–474.
- [12] Indurkha, Gopal, Rajurkar, K.P, 1992, Artificial Neural Network-approach in modeling of-EDM-process, *Intelligent Engineering Systems Through Artificial Neural Networks*, Volume 2, Pages 845-850



**M. K. Pradhan** is a Research Scholar at the Department. of Mechanical Engineering, N.I.T, Rourkela, India. He has over 10 years of teaching and research experience. His areas of research interest includes modeling and analysis of manufacturing processes and manufacturing optimisation. He has published more than 10 research papers in the International Journal / Conferences. He is a life member of ISTE, IACSIT and IE (I).